CAV-AHDV-CAV: Mitigating Traffic Oscillations for CAVs through a Novel Car-Following Structure and Reinforcement Learning

Xianda Chen, PakHin Tiu, Yihuai Zhang, Xinhu Zheng, Meixin Zhu

***Abstract*—Connected and Automated Vehicles (CAVs) offer a promising solution to the challenges of mixed traffic with both CAVs and Human-Driven Vehicles (HDVs). A significant hurdle in such scenarios is traffic oscillation, or the "stop-and-go" pattern, during car-following situations. While HDVs rely on limited information, CAVs can leverage data from other CAVs for better decision-making. This allows CAVs to anticipate and mitigate the spread of deceleration waves that worsen traffic flow. We propose a novel "CAV-AHDV-CAV" car-following framework that treats the sequence of HDVs between two CAVs as a single entity, eliminating noise from individual driver behaviors. This deep reinforcement learning approach analyzes vehicle equilibrium states and employs a state fusion strategy. Trained and tested on diverse datasets (HighD, NGSIM, SPMD, Waymo, Lyft) encompassing over 70,000 car-following instances, our model outperforms baselines in collision avoidance, maintaining equilibrium with both preceding and leading vehicles and achieving the lowest standard deviation of time headway. These results demonstrate the effectiveness of our approach in developing robust CAV control strategies for mixed traffic. Our model has the potential to mitigate traffic oscillation, improve traffic flow efficiency, and enhance overall safety.**

***Index Terms*—Traffic Oscillations, Mixed Traffic, Connected and Automated Vehicles, Human-Driven Vehicles, Deep Reinforcement Learning, Aggregated HDVs**

I. Introduction

TRAFFIC congestion, characterized by recurring periods of "stop-and-go" motion as shown in Fig. 1, plagues transportation systems globally. This phenomenon not only frustrates commuters but also incurs substantial economic and environmental burdens [1]–[4]. The emergence of Connected and Automated Vehicles (CAVs) presents a promising solution for mitigating traffic flow inefficiencies [5]–[8]. However, in mixed-traffic environments where CAVs coexist with Human-Driven Vehicles (HDVs), a critical challenge arises [9]–[11]. While CAV technology possesses the potential to revolutionize traffic management, the inherent unpredictability of HDV behavior significantly hinders the ability to fully harness this potential.

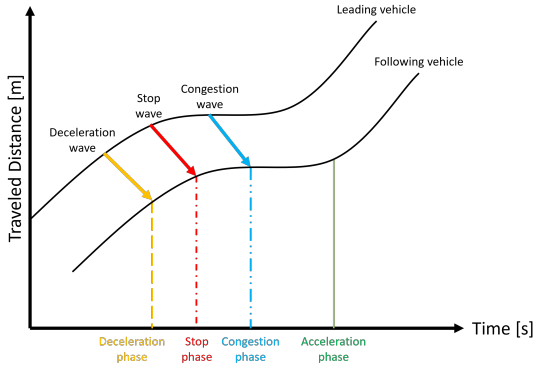

Fig. 1: Understanding traffic congestion: This diagram illustrates the deceleration wave and stop wave that contribute to traffic jams.

Building on the potential of CAVs, their advanced sensors and communication capabilities offer the ability to react more precisely and consistently to traffic conditions [12], [13]. This translates to smoother traffic flow, potentially eliminating the stop-and-go oscillations that plague current systems. These oscillations, characterized by repeated cycles of sudden braking and acceleration, significantly reduce traffic efficiency. Vehicles waste fuel while stuck in stop-and-go traffic, leading to increased emissions and environmental damage. Additionally, these rapid speed changes create safety hazards as drivers react poorly to unpredictable congestion [14], [15]. However, the success of CAV technology in achieving these improvements hinges on its ability to account for the unpredictable behavior of human drivers.

Unfortunately, directly implementing CAV control strategies in mixed traffic environments proves challenging due to the inherent variability in human driving behavior. Traditional car-following models struggle to account for sudden maneuvers, emotional responses, and other unpredictable actions of HDVs [16], [17]. This unpredictability disrupts the carefully planned maneuvers of CAVs, hindering their ability to optimize traffic flow. To address this gap, we propose the "CAV-AHDV-CAV" car-following framework as depicted in Fig. 2. This framework treats a sequence of HDVs following a leading CAV as a single, aggregated unit, termed the AHDV. By considering the

Xianda Chen and PakHin Tiu are co-first authors.

(*Corresponding author: Xinhu Zheng, Meixin Zhu*) Xianda Chen, PakHin Tiu, Yihuai Zhang, Xinhu Zheng and Meixin Zhu are with the Intelligent Transportation Thrust, The Hong Kong University of Science and Technology (Guangzhou), Guangzhou, 511400, China; Meixin Zhu and Xinhu Zheng are also with Guangdong Provincial Key Lab of Integrated Communication, Sensing and Computation for Ubiquitous Internet of Things (email: xchen595@connect.hkust-gz.edu.cn, phtiu454@connect.hkust-gz.edu.cn, yzhang169@connect.hkust-gz.edu.cn, xinhuzheng@hkust-gz.edu.cn, meixin@ust.hk). This study is supported by the National Natural Science Foundation of China under Grant 52302379 and 62373315, Guangzhou Basic and Applied Basic Research Projects under Grants 2023A03J0106, 2023A03J0683 and 2024A04J4290, Guangdong Province General Universities Youth Innovative Talents Project under Grant 2023KQNCX100, and Guangzhou Municipal Science and Technology Project 2023A03J0011.

AHDV's collective behavior, the following CAV can develop a more robust control strategy that mitigates the stop-and-go oscillations caused by individual HDV actions.

Our research aims to develop a control strategy for the following CAV within the "CAV-AHDV-CAV" framework. This strategy leverages real-time information collected by the leading CAV to predict the spread of traffic oscillations. Through Vehicle-to-Vehicle (V2V) communication, the following CAV receives information on the speed and spacing of the preceding AHDV and leading CAV, enabling it to adjust its actions accordingly. By effectively anticipating the AHDV's movements, the following CAV can proactively manage its speed and maintain a stable time headway, ultimately reducing the propagation of stop-and-go oscillations within the traffic flow.

This research offers several key contributions to the field of traffic flow management in mixed environments:

- **The "CAV-AHDV-CAV" framework:** We propose a novel car-following framework that treats a sequence of HDVs as an aggregated unit (AHDV), enabling the following CAV to account for collective behavior rather than individual, unpredictable actions.
- **Control strategy based on V2V communication:** The strategy utilizes real-time data from the leading CAV to predict AHDV behavior, allowing the following CAV to proactively adjust its speed and maintain a stable time headway.
- **Vehicle equilibrium states:** We introduce the concept of vehicle equilibrium states with the state fusion strategy, defining specific conditions for speed and spacing that optimize traffic flow within the framework.

The remainder of this paper is structured as follows. Section II delves into related work on traffic signal control and Autonomous Vehicle (AV) control strategies. Section III details our methodologies, outlining the assumptions made, the experimental setup, the concept of vehicle equilibrium, the state fusion formulation used to combine information, and the control strategy with its corresponding algorithms. Section IV describes the methodologies used for evaluation, including the dataset, implementation details, baseline models employed for comparison, and the results. Section V provides a discussion of the findings, and Section VI concludes the paper by summarizing the contributions and outlining future research directions.

II. Related Work

Several approaches have been explored to mitigate traffic oscillation, a recurring pattern of stop-and-go traffic flow. One approach focuses on optimizing traffic signal control [18], [19]. By strategically adjusting signal timings based on real-time traffic data, researchers aim to smooth traffic flow and prevent bottlenecks from forming, which can trigger oscillations. Another approach investigates the role of AV control. Proponents of this approach believe that vehicles equipped with advanced communication and control systems can coordinate their movements, maintaining a consistent speed and headway to prevent the propagation of disruptions and minimize oscillations.

A. Traffic Signal Control

One way to address the stop-and-go pattern of traffic congestion is by optimizing traffic signal control strategies. Aboudolas $el\ al.$ studied three traffic signal control methods for large congested urban networks, comparing their effectiveness and real-time applicability [20]. They also introduced a real-time traffic signal control system for congested cities that uses quadratic programming to optimize queue lengths and prevent gridlock [21]. Lo proposed a new traffic signal control system that adjusts to changing traffic conditions using real-time data and a comprehensive traffic flow model [22]. Atta $el\ al.$ suggested an adaptive traffic congestion control system utilizing RFID sensors and dynamic signal timing to ease traffic congestion [23]. Meanwhile, other researchers delved into network congestion control. Katabi $el\ al.$ introduced XCP, a new congestion control protocol designed to outperform TCP, especially in high-bandwidth and high-latency networks [24]. Hayes and Armitage presented a delay-gradient congestion control algorithm for TCP that enhances performance over traditional methods by reducing queuing delays and tolerating non-congestion-related packet losses [25]. Paganini $el\ al.$ proposed a congestion control system for general networks that achieves high performance, stability, and fairness; and allows for user preferences within a provably stable framework [26]. Mittal $el\ al.$ introduced a novel congestion control system for data centers that utilizes round-trip time (RTT) measurements for low-latency, high-bandwidth communication [27]. Mascolo proposed a congestion control algorithm for high-speed networks using Smith's principle to ensure stable data flow and efficient link utilization [28]. Cao $el\ al.$ suggested a delay-based congestion control algorithm for multipath TCP, achieving finer load balancing and faster congestion response compared to loss-based approaches [29]. However, these approaches rely on accurate data collection and traffic flow modeling, which can be challenging in real-world scenarios with unpredictable factors. Therefore, we aim to propose a microscopic autonomous vehicle control strategy that can adapt to these uncertainties and potentially improve traffic flow efficiency.

B. Autonomous Vehicle Control

Numerous studies in autonomous vehicle control have prioritized optimizing vehicle behavior to improve traffic flow. Chen $el\ al.$ introduced a car-following model that accurately reproduces stop-and-go traffic patterns by considering driver behavior and emphasizing the significance of analyzing microscopic traffic flow [30]. Zhou $el\ al.$ proposed a recurrent neural network model that effectively predicts traffic flow disruptions (oscillations) by capturing driver behavior more accurately than existing models [31]. He $el\ al.$ developed a data-driven car-following model that utilizes real-world traffic data and the k-nearest neighbor approach to predict vehicle behavior without relying on assumptions about driver behavior or fundamental diagrams [32]. They also suggested a "Jam-Absorption Driving (JAD)" strategy, where a designated vehicle slows down before traffic oscillations to eliminate them and enhance traffic flow [33]. However, these approaches have limitations

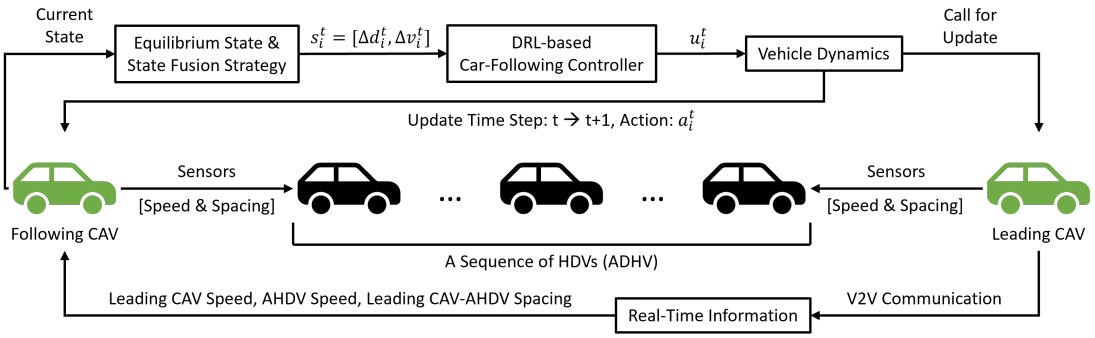

Fig. 2: "CAV-AHDV-CAV" car-following structure with deep reinforcement learning-based control.

as they mainly rely on predictions from a single vehicle's perspective, considering only the behavior of the car directly in front. By integrating information from a broader range of vehicles within a platoon, we can develop more precise predictions and potentially more effective control strategies. Hence, our proposed "CAV-AHDV-CAV" car-following structure aims to overcome this limitation in the existing model by addressing traffic oscillation mitigation. Additionally, we introduce a vehicle equilibrium state that takes into account both the preceding AHDV and the leading CAV, aiming to maintain a smooth acceleration based on the spacing and speed of these vehicles.

III. Methodology

A. Assumptions and Experimental Setup

This paper aims to develop advanced control strategies for CAVs in car-following scenarios within mixed traffic on an infinite one-lane segment. To enable a systematic analysis and focus on fundamental interactions, several crucial assumptions have been established:

i) CAVs are equipped with real-time information acquisition capabilities regarding the speed and position of surrounding vehicles;
ii) CAVs utilize V2V communication to exchange information with other CAVs in their vicinity;
iii) HDVs do not have communication capabilities and rely solely on their perception for situational awareness;
iv) Lane-changing maneuvers within the vehicular platoon are not considered, simplifying the analysis of the car-following process.

With these assumptions in place, our proposed "CAV-AHDV-CAV" car-following structure aims to address the interaction dynamics between CAVs and HDVs in a mixed-traffic scenario. As illustrated in Fig. 2, the leading CAV can acquire essential data such as its velocity, the velocity of the immediate following HDV, and the spacing between them. Similarly, the following CAV at the end of the convoy can gather information including its own velocity, the velocity of the immediate preceding HDV, and the spacing between them. Additionally, the following CAV has access to information transmitted by the leading CAV. Consequently, the HDVs located between the leading CAV and the following CAV can be treated as an aggregated vehicle unit, characterized by a time-variant vehicle length defined by the difference between the position of the head of the first HDV and the position of the tail of the last HDV in the sequence. Leveraging this aggregated unit characteristic, our proposed "CAV-AHDV-CAV" car-following structure can effectively ignore any lane-changing maneuvers within the AHDV sequence by focusing solely on the overall length of the sequence.

B. Vehicle Equilibrium

Upon establishing the conceptual framework for our proposed car-following model, this study draws inspiration from the concept of vehicle equilibrium state introduced in a prior work by Shi *et al.* [34]. The equilibrium state referred to here serves as a reference point for the following CAV (denoted as the i-th vehicle) to sustain an optimal relationship with both the preceding AHDV (denoted as the j-th vehicle) and the leading CAV (denoted as the k-th vehicle) in the platoon. This equilibrium state is characterized by two key elements: the equilibrium spacing denoted as $d_{m,n}^{*t}$ and the equilibrium velocity represented by $v_{m,n}^{*t}$. Importantly, this equilibrium state is dynamic and varies over time to adapt to the changing conditions at each time step.

The equilibrium spacing and velocity between the following CAV and the preceding AHDV are defined as follows:

$$d_{i,j}^{*t} = v_i^t \tau_i + l_i \tag{1}$$
$$v_{i,j}^{*t} = v_j^t \tag{2}$$

In the above equations, v_i^t and v_j^t represent the current velocity of the following CAV and the preceding AHDV, respectively. The parameters τ_i and l_i denote the desired constant time headway and the minimum standstill spacing between the following CAV and the preceding AHDV, respectively. With this equilibrium state, the following CAV aims to maintain a stable and harmonious interaction with the preceding AHDV.

Similarly, the equilibrium state between the following CAV and the leading CAV can be described as follows:

$$d_{i,k}^{*t} = v_i^t T_{i,k}^t + L_{i,k}^t \tag{3}$$
$$v_{i,k}^{*t} = v_k^t \tag{4}$$

Here, the time-dependent desired constant time headway $T_{i,k}^t$ and the minimum standstill spacing $L_{i,k}^t$ between the following

CAV and the leading CAV are calculated using the following equations:

$$T_{i,k}^t = \tau_i + T_{j,k}^t \tag{5}$$
$$L_{i,k}^t = l_i + L_{j,k}^t \tag{6}$$

The time-dependent desired constant time headway $T_{j,k}^t$ and the minimum standstill spacing $L_{j,k}^t$ between the preceding AHDV and the leading CAV, derived from Newell's car-following model [35], [36], can be calculated using the following equations:

$$T_{j,k}^t = \frac{d_{j,k}^t}{w + v_j^t} \tag{7}$$
$$L_{j,k}^t = wT_{j,k}^t \tag{8}$$

Here, the parameter w represents the wave speed, which refers to the speed at which disturbances or waves travel through a line of vehicles.

To further elaborate on the concept of vehicle equilibrium and its dynamic nature, we introduce the deviation function, which is derived from the equilibrium spacing and velocity equations. The deviation functions are defined as follows:

$$\Delta d_{i,j/k}^t = d_{i,j/k}^t - d_{i,j/k}^{*t} \tag{9}$$
$$\Delta v_{i,j/k}^t = v_i^t - v_i^{*t} \tag{10}$$

C. State Fusion Formulation

In our proposed "CAV-AHDV-CAV" car-following framework, the following CAV incorporates information not only from the preceding AHDV but also from the leading CAV to mitigate traffic oscillations. To achieve this, we introduce a novel state fusion strategy that integrates the equilibrium states associated with both the preceding AHDV and the leading CAV. This fusion strategy empowers the following CAV to dynamically adjust its spacing and velocity, ensuring the maintenance of an optimal state relative to both the preceding AHDV and the leading CAV within the traffic flow system.

The fusion state of the following CAV is determined using the following equations:

$$\Delta d_i^t = \frac{q_j \Delta d_{i,j}^t + q_k \Delta d_{i,k}^t}{q_j + q_k} \tag{11}$$
$$\Delta v_i^t = \frac{q_j \Delta v_{i,j}^t + q_k \Delta v_{i,k}^t}{q_j + q_k} \tag{12}$$

where q_j and q_k are the weights assigned to the two equilibrium states, determining their influence on the fusion state of the following CAV. By appropriately assigning these weights, a balanced fusion state can be achieved, incorporating the best aspects of each equilibrium.

D. Control Strategy and Algorithms

Upon the implementation of the state fusion strategy to achieve vehicle equilibrium, the current state return values can be derived as $s_i^t = [\Delta d_i^t, \Delta v_i^t]$. Additionally, an action a_i^t is determined by the agent to represent the acceleration at the current time step. To assess the system's performance based on the current state and action, it is necessary to define a reward function r_i^t. This reward function quantitatively measures the system's performance and provides feedback to the learning algorithm, thereby guiding the agent towards making decisions that lead to the equilibrium state within our car-following framework.

In our proposed framework, the reward function is defined as follows:

$$r_i^t = \exp(-(c_i^t + g_i^t)) \tag{13}$$

where

$$c_i^t = (s_i^t)^T \begin{bmatrix} \alpha_{1,i} & 0 \\ 0 & \alpha_{2,i} \end{bmatrix} s_i^t \tag{14}$$
$$g_i^t = \alpha_{3,i}(a_i^t)^2 \tag{15}$$

Here, the adjustable weights $\alpha_{1,i}$, $\alpha_{2,i}$, and $\alpha_{3,i}$ can be determined using the same settings employed in the optimal control method.

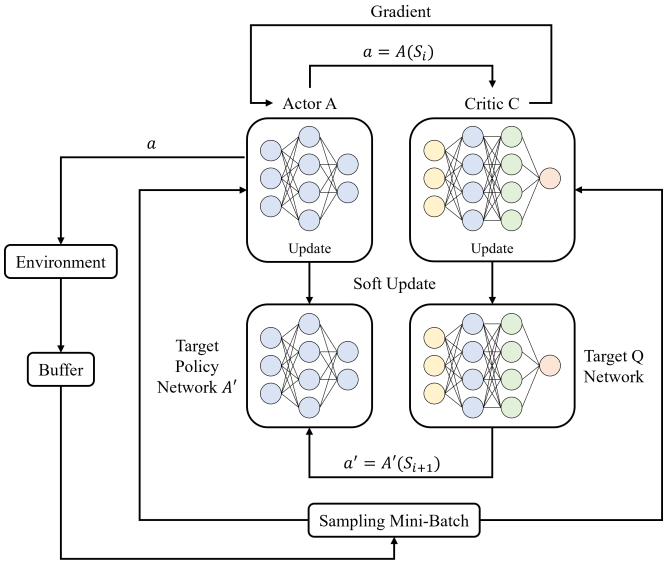

Fig. 3: Illustration of the intricate architecture and components of the Deep Deterministic Policy Gradient (DDPG) algorithm.

After defining the reward function in our car-following framework, we incorporated the Deep Deterministic Policy Gradient (DDPG) algorithm, as suggested by Lillicrap *el al.* [37], to aid learning and improve decision-making. Illustrated in Fig. 3, the DDPG algorithm is a model-free, off-policy reinforcement learning method well-suited for continuous action spaces, making it ideal for handling the intricacies of our car-following system. DDPG comprises two main components: the Actor and the Critic networks. The Actor network directly learns the optimal policy by mapping states s_i^t to actions a_i^t, providing continuous control outputs. In contrast, the Critic network assesses the actions a_i^t chosen by the Actor by estimating the Q-value function, enhancing learning by offering feedback on the selected actions. Furthermore, the integration of target Actor and target Critic networks in DDPG enhances training stability. These target networks help address issues like overestimation or divergence during training by gradually updating target values, leading to more consistent and effective learning outcomes.

IV. Experiments

A. Dataset

In this study, we implemented the data selection criteria as detailed in our prior work [38]. This process involved the utilization of five distinct datasets: HighD [39], NGSIM [40], SPMD [41], Waymo [42], and Lyft [43]. Notably, the HighD dataset presented a recording frame rate of 25Hz, differing from the 10Hz frame rate observed in the remaining datasets. To ensure consistency during training and avoid episode length variations, we standardized all car-following pairs to a fixed duration. Each event became precisely 10 seconds long, corresponding to 250 frames in the HighD dataset and 100 frames in other datasets.

Our analysis identified a total of $76,553$ car-following pairs across the datasets. Specifically, the HighD dataset contributed $12,540$ car-following pairs, the NGSIM dataset contained $1,725$ pairs, the SPMD dataset (SPMD1 and SPMD2) included $40,903$ pairs, the Waymo dataset featured 661 pairs, and the Lyft dataset comprised $20,724$ pairs. Following the established protocol, we partitioned the collected data into a training set (70%) and a testing set (30%). Each car-following pair includes four types of extracted data: the spacing between the following vehicle and the leading vehicle, the speed of the following vehicle and the leading vehicle, and the relative speed between them.

To fit our proposed "CAV-AHDV-CAV" car-following structure, we treated the car-following pair as the leading CAV and the preceding AHDV. We simulated the following CAV with an initial state where the initial spacing and speed of the following CAV were determined based on the preceding AHDV and the leading CAV as follows:

$$v_i^0 = \frac{v_j^0 + v_k^0}{2} \tag{16}$$

$$d_{i,j}^0 = d_{j,k}^0 \tag{17}$$

where v_j^0 and v_k^0 represents the initial speed of the preceding AHDV and the leading CAV, respectively.

B. Implementation

This study uses Stable-Baselines3 (SB3) [44], a Python library offering user-friendly implementations of various reinforcement learning (RL) algorithms. Built on top of PyTorch, a popular framework for deep learning and deep reinforcement learning (DRL), SB3 simplifies our development process. In our car-following environment, we set a constant acceleration limit of 3m/s^2 and defined the action space to range from -3m/s^2 to 3m/s^2. We also established specific parameters for the desired constant time headway τ_i and minimum standstill spacing l_i at 0.85s and 2.3m (half of the vehicle length), respectively. The wave speed was set to 4.4m/s. The reset function within our car-following environment initializes the following CAV as defined in Eq. 16 and Eq. 17. It then combines this information to create an initial fusion state that's returned by the function. The step function takes an action (acceleration in our case) as input and updates the state of the following CAV. It then calculates a new fusion state based on this updated state. This new fusion state, along with a reward (as defined in Eq. 13), a termination signal (`True`/`False`), and the history of rewards, are all returned by the step function.

Our training process relies on a specific type of policy network architecture called "MlpPolicy." This architecture utilizes Multi-Layer Perceptrons (MLPs), which are essentially artificial neural networks with at least three hidden layers. Each layer consists of fully connected neurons that employ a non-linear activation function. This non-linearity is crucial because it allows the network to learn complex relationships between the input data (the vehicle's state) and the desired output (optimal acceleration). Cybenko's work in 1989 [45] demonstrated that MLPs have the exceptional capability to differentiate patterns in data that linear models are unable to separate.

For the optimization of the training process, we meticulously chose various hyperparameters. The batch size, defining the number of data points utilized for updating the network weights in each training step, is configured to 16. The learning rate, which controls how much the network adjusts its weights based on the learning signal, is set to 0.0001. Finally, the total training time step, which defines the number of times the agent interacts with the environment and learns from the experience, is set to $200,000$. Additionally, we set the random seed to 42. This ensures that if the training process is run again with the same settings, it will produce the same results, allowing for reproducibility of our experiments.

C. Baseline Models

In order to assess the effectiveness of our model, we carried out a thorough evaluation by comparing it against several established car-following models. These models included the Intelligent Driver Model (IDM) developed by Treiber $el\ al.$ [46], a Neural Network (NN)-based model, and a Long Short-Term Memory (LSTM)-based model. However, in our experiment settings of these existing models, the following CAV lacks access to information from the leading CAV. Consequently, the following CAV makes decisions based solely on its own data and the information gathered from the preceding AHDV through its sensors.

The IDM represents a fundamental and widely accepted traditional car-following model that is extensively utilized in various research endeavors. It serves as a fundamental basis for understanding and simulating driver behaviors in traffic scenarios, providing a crucial benchmark for evaluating the performance of newer car-following models. Within our framework, we defined the comfortable acceleration as 1m/s^2. Additionally, the desired speed reflects the equilibrium states of speed and spacing relative to the preceding AHDV, as outlined in Eq. 1 and Eq. 2. In our model setup, we have configured the beta parameter to be 2, enabling the model to achieve the desired speed and spacing equally. Furthermore, we have constrained the acceleration output within the range of $[-3, 3]$, ensuring realistic and bounded acceleration values for the simulation.

On the contrary, the NN-based model comprises three fully connected layers with Rectified Linear Unit (ReLU) activation functions interposed between them, culminating in a final

linear layer with a hyperbolic tangent activation function. The LSTM-based model processes the input through three hidden layers followed by a linear layer with a hyperbolic tangent activation function. At each time step, the inputs pertain to the current state of the following CAV and the preceding AHDV without any information regarding the leading CAV. The model generates an acceleration value constrained within the range of $[-3, 3]$. Both models undergo training using the complete training dataset with identical learning rates and batch sizes as employed in our DDPG model. The loss function for both models is delineated as the Mean Square Error (MSE) between the speed of the current state and the equilibrium state concerning the preceding AHDV as described in Eq. 1 and Eq. 2, incorporating an additional penalty for collisions and reverse movements.

D. Evaluation Metrics

In our experimental setup, which integrates learning-based models such as NN, LSTM networks, and DDPG algorithms, it is essential to evaluate the proficiency of these models in collision avoidance. One key evaluation metric for our learning-based models is the collision rate, which is defined as:

$$\text{Collision Rate} = \frac{\text{Number of Events with Spacing} < 0}{\text{Total Number of Car-Following Events}} \tag{18}$$

After establishing equilibrium states for the following CAV concerning both the preceding AHDV and the leading CAV, a fundamental evaluation measure is the MSE that quantifies the disparity between the simulated state and the equilibrium state. The MSE for each occurrence is expressed as:

$$\text{MSE} = \frac{1}{N}\sum_{t=0}^{T}(S^t - S^{*t})^2 \tag{19}$$

where N signifies the total number of time steps, t denotes the index of the time step, S^t represents the simulated state at time step t, and S^{*t} corresponds to the equilibrium state at time step t. Our experiments evaluated the model's performance using three equilibrium states: the fused equilibrium state for speed, and separate equilibrium states for spacing with both the preceding AHDV and the leading CAV.

Additionally, our proposed model is tailored to address traffic oscillations. To evaluate the impact of different control models on these oscillations, we introduce the concept of string stability within the platoon. This approach enables us to measure how various control models affect traffic oscillations. In the absence of a standardized evaluation metric for traffic oscillation, we define our own metric as the standard deviation of the time headway of the following CAV concerning both the preceding AHDV and the leading CAV.

To compute the time headway at each time step, we employ the following formula:

$$\text{THW}_{i,j}^t = \frac{d_{i,j}^t}{v_i^t} \tag{20}$$

Here, $\text{THW}_{i,j}^t$ represents the time headway between the following CAV and the preceding AHDV at time t. We can similarly calculate the time headway between the following CAV and the leading CAV.

Subsequently, to determine the standard deviation of time headway of the n-th event, we utilize the following equation:

$$\mu_{i,j}^n = \frac{1}{T}\sum_{t=0}^{T}(\text{THW}_{i,j}^t - \bar{\text{THW}}_{i,j})^2 \tag{21}$$

where T represents the total number of time steps of the n-th event and $\bar{\text{THW}}_{i,j}$ denotes the average time headway throughout the entire event.

E. Results

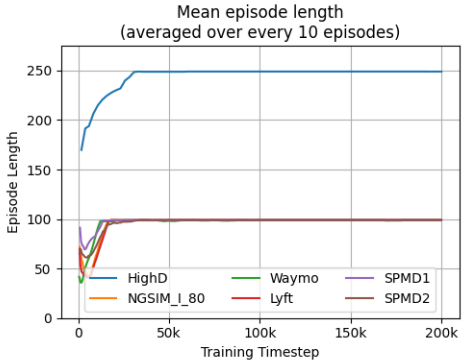

(a) Mean episode length (averaged over every 10 episodes).

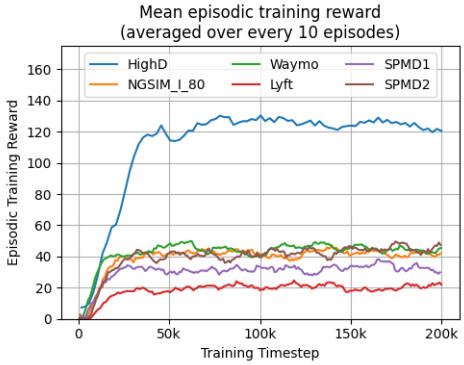

(b) Mean episodic training reward (averaged over every 10 episodes).

Fig. 4: DRL training progress across all datasets.

Upon completing the training of our DDPG-based model across all datasets, we observed successful convergence of reward values in each training episode. Moreover, the episode length consistently reached the final time step for every event, as illustrated in Fig. 4. Notably, the trend depicted in Fig. 4a demonstrates a positive trajectory post $200,000$ time steps, indicating the agent's progressive mastery of achieving objectives without encountering issues such as collisions, backward movements, or stalling scenarios. Instances of these undesirable behaviors would prompt the assignment of a reward value of 0, leading to an immediate termination of the ongoing training episode. Consequently, the agent would fail to progress towards reaching the final time step. It is noteworthy

that the episodic training reward of each dataset converged to a unique value corresponding to the characteristics of that dataset. Figure 4b shows the episodic training reward across different datasets. The reward for the HighD dataset reaches the highest value, converging around 120. Conversely, the Lyft dataset exhibits the lowest reward, converging around 20.

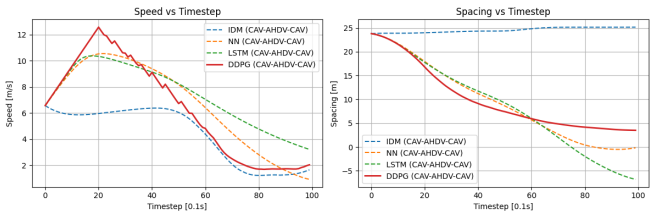

(a) Event 1.

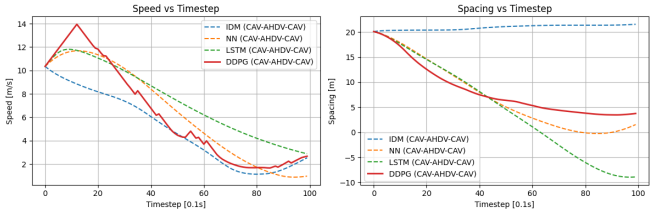

(b) Event 2.

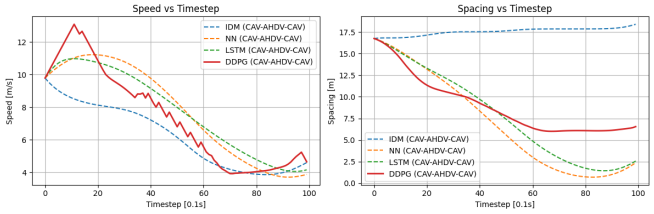

(c) Event 3.

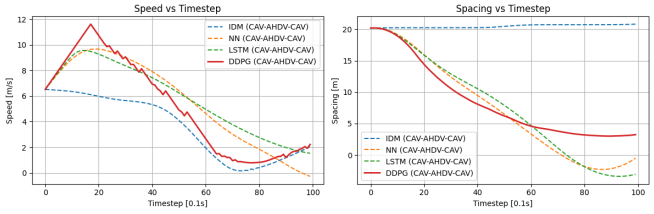

(d) Event 4.

Fig. 5: Comparisons of speed and spacing controlled by our proposed model and the baseline models (IDM, NN-based, and LSTM-based) across 4 randomly selected events.

To visualize our proposed model's control strategies compared to baselines, we randomly selected four stop-and-go events from the testing dataset. Fig. 5 presents the results. Here, bold red solid lines represent our model, while blue dashed, orange dashed, and green dashed lines depict IDM, NN-based, and LSTM-based models, respectively. The figure has two plots: the left plot is the speed control of different models; the right plot is the corresponding spacing resulting from the speed control. Fig. 6 showcases the simulated trajectories of the following CAV by each model. For reference, preceding AHDV and leading CAV trajectories are shown in purple and brown solid lines, respectively. Table I summarizes the overall performance of each model across different datasets. It presents the results for our defined evaluation metrics, including collision rates, MSEs in speed and spacing, and the mean standard deviation of time headway. Additionally, the table includes an average of all the results, providing a comprehensive comparison of the models' overall performance.

V. Discussion

A. Results Analysis

Fig. 5 and Fig. 6 reveal distinct behaviors of the compared models in all four randomly chosen events. The IDM strategy maintained a larger following distance from the preceding AHDV by simply matching its speed. In contrast, the NN-based, LSTM-based, and our proposed model all initiated deceleration to reach a stable equilibrium state. Here's the key difference:

- The NN-based and LSTM-based models focused solely on achieving equilibrium with the preceding AHDV.
- Our proposed model, however, considered both the preceding AHDV and the leading CAV, incorporating a balance as defined in Eq. 11 and Eq. 12. This enabled it to anticipate the deceleration of the preceding AHDV by considering the leading CAV's influence. Consequently, when the leading CAV slowed down, our model reacted proactively, avoiding collisions or near-collisions, unlike the NN-based and LSTM-based models that reacted only after the preceding AHDV braked.

These results demonstrate the advantage of our proposed model in handling stop-and-go scenarios compared to baseline models (IDM, NN-based, LSTM-based). By considering both the preceding AHDV and the leading CAV, our model can anticipate upcoming changes and react proactively, achieving smoother and safer interactions within the traffic flow.

The performance evaluation in Table I further strengthens the advantages of our proposed model. It demonstrates significant improvements in collision avoidance compared to baseline models. Notably, our model achieves a remarkably low overall collision rate of 0.048%, far exceeding the NN-based model (2.138%) and LSTM-based model (4.297%). This translates to zero collisions in both the HighD and NGSIM (I-80) datasets. While IDM excels at achieving a desired speed (resulting in the lowest overall MSE of speed at 4.938), our proposed model achieves a competitive overall MSE of speed (19.272) while significantly outperforming the NN-based and LSTM-based models. It's worth noting that our model achieves the best overall MSE of speed (2.977) in the HighD dataset. In terms of maintaining spacing, all three models (NN-based, LSTM-based, and ours) demonstrate similar performance regarding the preceding AHDV (around 490 MSE). However, our proposed model shines in maintaining equilibrium with both the preceding AHDV and the leading CAV, achieving the lowest overall MSE of spacing concerning the leading CAV (311.035). This advantage is further emphasized by the IDM's significantly higher MSEs in spacing. The mean standard deviations of time headway follow a similar trend. While IDM exhibits the highest overall values, our proposed model achieves the lowest concerning the preceding AHDV

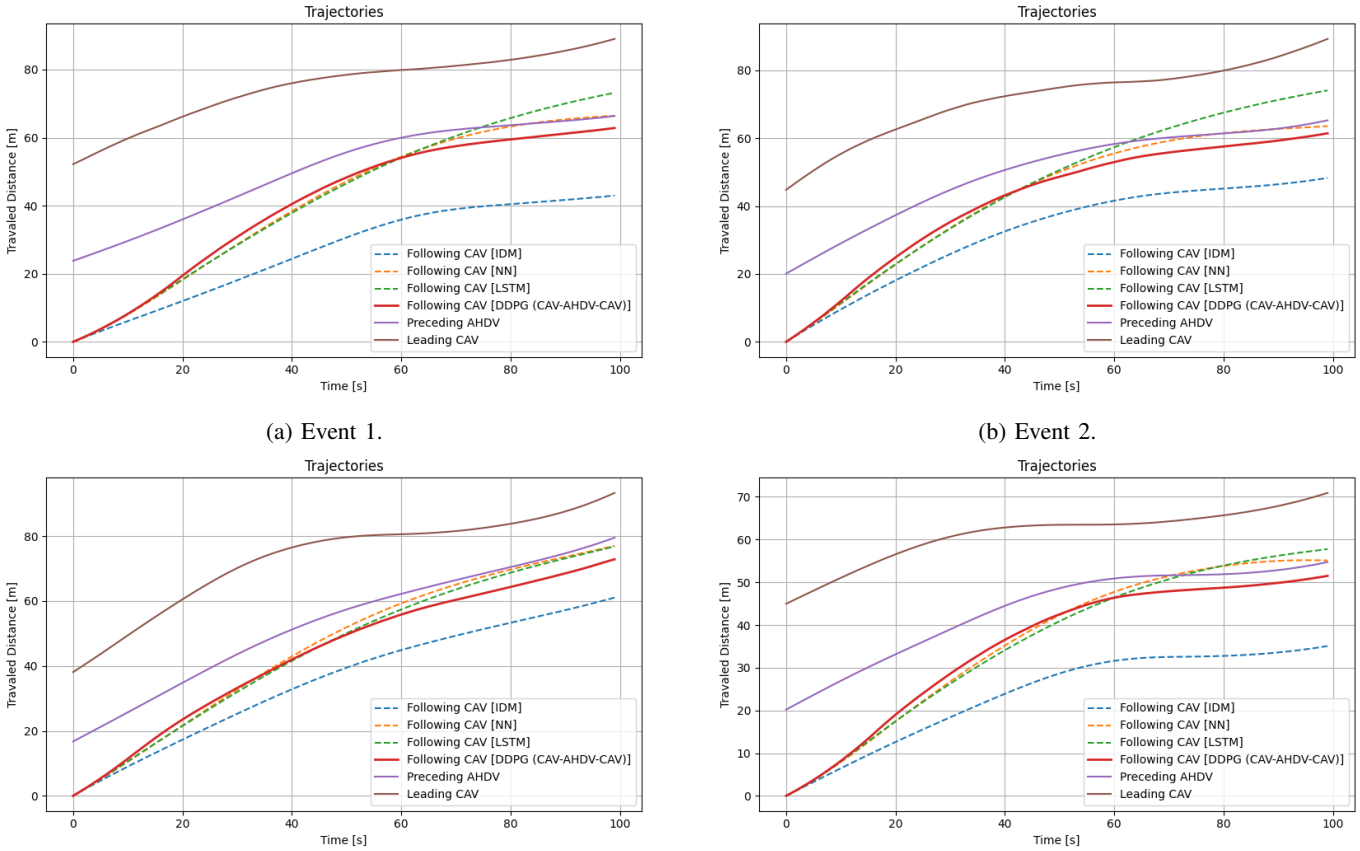

(a) Event 1.

(b) Event 2.

(c) Event 3.

(d) Event 4.

Fig. 6: Comparisons of simulated trajectories by our proposed model and the baseline models (IDM, NN-based, and LSTM-based) with references of the trajectories of the preceding AHDV and the leading CAV across 4 randomly selected events.

(0.539), outperforming the NN-based (0.645) and LSTM-based (0.613) models. While the LSTM-based model achieves a slightly lower overall value (0.905) regarding the leading CAV, our model's performance remains highly competitive (0.930). Overall, these results demonstrate the effectiveness of our proposed model in stop-and-go scenarios. By considering both preceding and leading vehicles, it achieves superior performance in collision avoidance, equilibrium state maintenance, and smoother interactions within the traffic flow.

B. Limitations

While our proposed model has shown promise in helping CAVs reduce the impact of traffic oscillation in mixed traffic by leveraging information from the leading CAV and predicting stop-and-go patterns for early braking and maintaining the movement without dropping the speed to 0, there are limitations in our experimental setup that need to be considered. Firstly, in our experiments, we treat a sequence of HDVs as an aggregated unit, but we only have one vehicle between the CAVs in our setup. To validate our assumption that treating a sequence of HDVs as an aggregated unit can eliminate the variability of HDVs, further validation on car-following events with varying numbers of HDVs is necessary. Secondly, our car-following platoon consists of only two CAVs, whereas in real-world scenarios, multiple CAVs can work together to address traffic oscillation. Future research could explore more complex variants, such as CAV-AHDV-CAV-AHDV-CAV, or involve a greater number of CAVs in the platoon. Lastly, our results are based on simulation validation and lack support from real-world traffic data. Moving forward, it is essential to enhance real-world implementation to validate the effectiveness of our model in practical traffic scenarios.

VI. Conclusion

In conclusion, our study introduces a CAV-AHDV-CAV car-following framework employing deep reinforcement learning to tackle traffic oscillations in mixed traffic scenarios. This structure effectively addresses the stochastic behaviors of HDVs during car-following events by aggregating a sequence of HDVs. Leveraging V2V communication capabilities, our framework integrates a vehicle equilibrium state and state fusion strategy, enabling the following CAV to make decisions based on the preceding AHDV and the leading CAV. Through extensive training and testing on diverse datasets such as HighD, NGSIM, SPMD, Waymo, and Lyft, our model demonstrates superior performance in collision prevention, achieving equilibrium states, and maintaining stable time headways. These results underscore the effectiveness of our proposed approach in addressing dynamic traffic challenges across various scenarios. Future research endeavors could focus on enhancing

TABLE I: Comparison of performance metrics between our proposed model and baseline models in different datasets, focusing on collision rate, mean squared error in speed and spacing, and mean standard deviation of time headway.

Dataset	Model	Collision Rate	Speed MSE	Spacing MSE (Preceding AHDV)	Spacing MSE (Leading CAV)	THW STD (Preceding AHDV)	THW STD (Leading CAV)
HighD	IDM	0	5.675	933.653	1042.102	0.511	0.557
	NN	4.386%	7.884	**104.286**	100.108	0.283	0.342
	LSTM	7.230%	8.095	134.325	131.020	0.298	0.374
	Proposed Model	**0**	**2.977**	120.574	**68.848**	**0.141**	**0.197**
NGSIM (I-80)	IDM	0	**1.176**	467.868	499.176	0.625	1.177
	NN	0.772%	8.607	80.796	68.663	0.448	0.942
	LSTM	0.965%	7.547	82.548	**59.606**	**0.417**	**0.786**
	Proposed Model	**0**	8.579	**78.211**	60.184	**0.419**	0.893
SPMD1	IDM	0	**6.207**	2262.288	2473.656	0.487	**0.716**
	NN	0.941%	22.378	402.268	326.743	0.522	0.798
	LSTM	1.981%	21.088	410.275	326.616	0.496	0.771
	Proposed Model	**0.060%**	19.936	**399.323**	**274.632**	**0.467**	0.758
SPMD2	IDM	0	**6.327**	1572.982	1739.531	0.488	**0.547**
	NN	0.192%	13.547	209.784	155.990	0.294	0.417
	LSTM	0.206%	12.335	213.245	149.735	0.273	0.394
	Proposed Model	**0.041%**	13.291	**205.000**	**141.299**	**0.266**	0.401
Waymo	IDM	0	**7.564**	7688.743	8410.795	13.997	29.539
	NN	2.513%	8.801	84.620	72.731	1.755	8.416
	LSTM	5.025%	7.658	88.630	64.418	1.060	**2.186**
	Proposed Model	**0.050%**	8.338	**80.653**	**58.622**	**0.098**	2.408
Lyft	IDM	0	**2.078**	4080.680	4194.535	14.679	25.371
	NN	4.117%	46.312	**1142.874**	1457.524	1.356	2.421
	LSTM	9.424%	44.133	1165.577	1424.913	1.296	**1.899**
	Proposed Model	**0.080%**	36.837	1171.969	**788.261**	**1.183**	2.086
Overall	IDM	0	**4.938**	2325.159	2479.441	4.453	7.571
	NN	2.138%	23.258	**482.987**	533.636	0.645	1.111
	LSTM	4.297%	22.004	496.965	527.586	0.613	**0.905**
	Proposed Model	**0.048%**	19.272	491.282	**311.035**	**0.539**	0.930

the scalability and generalization of our model by validating its effectiveness and efficiency in real-world settings.vvvv

REFERENCES

[1] X. Li, J. Cui, S. An, and M. Parsafard, "Stop-and-go traffic analysis: Theoretical properties, environmental impacts and oscillation mitigation," *Transportation Research Part B: Methodological*, vol. 70, pp. 319–339, 2014.

[2] S. Oh and H. Yeo, "Impact of stop-and-go waves and lane changes on discharge rate in recovery flow," *Transportation Research Part B: Methodological*, vol. 77, pp. 88–102, 2015.

[3] Y. Li, Z. Li, H. Wang, W. Wang, and L. Xing, "Evaluating the safety impact of adaptive cruise control in traffic oscillations on freeways," *Accident Analysis & Prevention*, vol. 104, pp. 137–145, 2017.

[4] Z. Zheng, S. Ahn, and C. M. Monsere, "Impact of traffic oscillations on freeway crash occurrences," *Accident Analysis & Prevention*, vol. 42, no. 2, pp. 626–636, 2010.

[5] J. Guanetti, Y. Kim, and F. Borrelli, "Control of connected and automated vehicles: State of the art and future challenges," *Annual reviews in control*, vol. 45, pp. 18–40, 2018.

[6] D. Elliott, W. Keen, and L. Miao, "Recent advances in connected and automated vehicles," *journal of traffic and transportation engineering (English edition)*, vol. 6, no. 2, pp. 109–131, 2019.

[7] A. Vahidi and A. Sciarretta, "Energy saving potentials of connected and automated vehicles," *Transportation Research Part C: Emerging Technologies*, vol. 95, pp. 822–843, 2018.

[8] S. E. Shladover, "Connected and automated vehicle systems: Introduction and overview," *Journal of Intelligent Transportation Systems*, vol. 22, no. 3, pp. 190–200, 2018.

[9] W.-X. Zhu and H. M. Zhang, "Analysis of mixed traffic flow with human-driving and autonomous cars based on car-following model," *Physica A: Statistical Mechanics and its Applications*, vol. 496, pp. 274–285, 2018.

[10] M. Al-Turki, N. T. Ratrout, S. M. Rahman, and I. Reza, "Impacts of autonomous vehicles on traffic flow characteristics under mixed traffic environment: Future perspectives," *Sustainability*, vol. 13, no. 19, p. 11052, 2021.

[11] C. R. Munigety and T. V. Mathew, "Towards behavioral modeling of drivers in mixed traffic conditions," *Transportation in Developing Economies*, vol. 2, pp. 1–20, 2016.

[12] A. Sarker, H. Shen, M. Rahman, M. Chowdhury, K. Dey, F. Li, Y. Wang, and H. S. Narman, "A review of sensing and communication, human factors, and controller aspects for information-aware connected and automated vehicles," *IEEE transactions on intelligent transportation systems*, vol. 21, no. 1, pp. 7–29, 2019.

[13] W. Yuan, Z. Wei, S. Li, J. Yuan, and D. W. K. Ng, "Integrated sensing and communication-assisted orthogonal time frequency space transmission for vehicular networks," *IEEE Journal of Selected Topics in Signal Processing*, vol. 15, no. 6, pp. 1515–1528, 2021.

[14] R. B. Noland and M. A. Quddus, "Congestion and safety: A spatial analysis of london," *Transportation Research Part A: Policy and Practice*, vol. 39, no. 7-9, pp. 737–754, 2005.

[15] D. Shefer and P. Rietveld, "Congestion and safety on highways: towards an analytical model," *Urban Studies*, vol. 34, no. 4, pp. 679–692, 1997.

[16] J. Sun, Z. Zheng, and J. Sun, "Stability analysis methods and their applicability to car-following models in conventional and connected environments," *Transportation research part B: methodological*, vol. 109, pp. 212–237, 2018.

[17] M. Saifuzzaman and Z. Zheng, "Incorporating human-factors in car-following models: a review of recent developments and research needs," *Transportation research part C: emerging technologies*, vol. 48, pp. 379–403, 2014.

[18] S. H. Low, F. Paganini, and J. C. Doyle, "Internet congestion control," *IEEE control systems magazine*, vol. 22, no. 1, pp. 28–43, 2002.

[19] S. Ryu, C. Rump, and C. Qiao, "Advances in internet congestion control," *IEEE Communications Surveys & Tutorials*, vol. 5, no. 1, pp. 28–39, 2003.

[20] K. Aboudolas, M. Papageorgiou, and E. Kosmatopoulos, "Store-and-forward based methods for the signal control problem in large-scale con-

gested urban road networks," *Transportation Research Part C: Emerging Technologies*, vol. 17, no. 2, pp. 163–174, 2009.
[21] K. Aboudolas, M. Papageorgiou, A. Kouvelas, and E. Kosmatopoulos, "A rolling-horizon quadratic-programming approach to the signal control problem in large-scale congested urban road networks," *Transportation Research Part C: Emerging Technologies*, vol. 18, no. 5, pp. 680–694, 2010.
[22] H. K. Lo, "A novel traffic signal control formulation," *Transportation Research Part A: Policy and Practice*, vol. 33, no. 6, pp. 433–448, 1999.
[23] A. Atta, S. Abbas, M. A. Khan, G. Ahmed, and U. Farooq, "An adaptive approach: Smart traffic congestion control system," *Journal of King Saud University-Computer and Information Sciences*, vol. 32, no. 9, pp. 1012–1019, 2020.
[24] D. Katabi, M. Handley, and C. Rohrs, "Congestion control for high bandwidth-delay product networks," in *Proceedings of the 2002 conference on Applications, technologies, architectures, and protocols for computer communications*, 2002, pp. 89–102.
[25] D. A. Hayes and G. Armitage, "Revisiting tcp congestion control using delay gradients," in *International Conference on Research in Networking*. Springer, 2011, pp. 328–341.
[26] F. Paganini, Z. Wang, J. C. Doyle, and S. H. Low, "Congestion control for high performance, stability, and fairness in general networks," *IEEE/ACM Transactions On Networking*, vol. 13, no. 1, pp. 43–56, 2005.
[27] R. Mittal, V. T. Lam, N. Dukkipati, E. Blem, H. Wassel, M. Ghobadi, A. Vahdat, Y. Wang, D. Wetherall, and D. Zats, "Timely: Rtt-based congestion control for the datacenter," *ACM SIGCOMM Computer Communication Review*, vol. 45, no. 4, pp. 537–550, 2015.
[28] S. Mascolo, "Congestion control in high-speed communication networks using the smith principle," *Automatica*, vol. 35, no. 12, pp. 1921–1935, 1999.
[29] Y. Cao, M. Xu, and X. Fu, "Delay-based congestion control for multipath tcp," in *2012 20th IEEE international conference on network protocols (ICNP)*. IEEE, 2012, pp. 1–10.
[30] D. Chen, J. Laval, Z. Zheng, and S. Ahn, "A behavioral car-following model that captures traffic oscillations," *Transportation research part B: methodological*, vol. 46, no. 6, pp. 744–761, 2012.
[31] M. Zhou, X. Qu, and X. Li, "A recurrent neural network based microscopic car following model to predict traffic oscillation," *Transportation research part C: emerging technologies*, vol. 84, pp. 245–264, 2017.
[32] Z. He, L. Zheng, and W. Guan, "A simple nonparametric car-following model driven by field data," *Transportation Research Part B: Methodological*, vol. 80, pp. 185–201, 2015.
[33] Z. He, L. Zheng, L. Song, and N. Zhu, "A jam-absorption driving strategy for mitigating traffic oscillations," *IEEE Transactions on Intelligent Transportation Systems*, vol. 18, no. 4, pp. 802–813, 2016.
[34] H. Shi, Y. Zhou, K. Wu, X. Wang, Y. Lin, and B. Ran, "Connected automated vehicle cooperative control with a deep reinforcement learning approach in a mixed traffic environment," *Transportation Research Part C: Emerging Technologies*, vol. 133, p. 103421, 2021.
[35] G. F. Newell, "A simplified theory of kinematic waves in highway traffic, part i: General theory," *Transportation Research Part B: Methodological*, vol. 27, no. 4, pp. 281–287, 1993.
[36] ——, "A simplified car-following theory: a lower order model," *Transportation Research Part B: Methodological*, vol. 36, no. 3, pp. 195–205, 2002.
[37] T. P. Lillicrap, J. J. Hunt, A. Pritzel, N. Heess, T. Erez, Y. Tassa, D. Silver, and D. Wierstra, "Continuous control with deep reinforcement learning," *arXiv preprint arXiv:1509.02971*, 2015.
[38] X. Chen, M. Zhu, K. Chen, P. Wang, H. Lu, H. Zhong, X. Han, X. Wang, and Y. Wang, "Follownet: A comprehensive benchmark for car-following behavior modeling," *Scientific data*, vol. 10, no. 1, p. 828, 2023.
[39] R. Krajewski, J. Bock, L. Kloeker, and L. Eckstein, "The highd dataset: A drone dataset of naturalistic vehicle trajectories on german highways for validation of highly automated driving systems," in *2018 21st international conference on intelligent transportation systems (ITSC)*. IEEE, 2018, pp. 2118–2125.
[40] "Next generation simulation (ngsim) vehicle trajectories and supporting data," *ITS DataHub through Data.transportation.gov.* http://doi.org/10.21949/1504477, 2016.
[41] D. Bezzina and J. Sayer, "Safety pilot model deployment: Test conductor team report," *Report No. DOT HS*, vol. 812, no. 171, p. 18, 2014.
[42] P. Sun, H. Kretzschmar, X. Dotiwalla, A. Chouard, V. Patnaik, P. Tsui, J. Guo, Y. Zhou, Y. Chai, B. Caine *et al.*, "Scalability in perception for autonomous driving: Waymo open dataset," in *Proceedings of the IEEE/CVF conference on computer vision and pattern recognition*, 2020, pp. 2446–2454.
[43] J. Houston, G. Zuidhof, L. Bergamini, Y. Ye, L. Chen, A. Jain, S. Omari, V. Iglovikov, and P. Ondruska, "One thousand and one hours: Self-driving motion prediction dataset," in *Conference on Robot Learning*. PMLR, 2021, pp. 409–418.
[44] A. Raffin, A. Hill, A. Gleave, A. Kanervisto, M. Ernestus, and N. Dormann, "Stable-baselines3: Reliable reinforcement learning implementations," *The Journal of Machine Learning Research*, vol. 22, no. 1, pp. 12 348–12 355, 2021.
[45] G. Cybenko, "Approximation by superpositions of a sigmoidal function," *Mathematics of control, signals and systems*, vol. 2, no. 4, pp. 303–314, 1989.
[46] M. Treiber, A. Hennecke, and D. Helbing, "Congested traffic states in empirical observations and microscopic simulations," *Physical review E*, vol. 62, no. 2, p. 1805, 2000.

Xianda Chen received the M.S. degree from The University of Hong Kong, Hong Kong, China, in 2022. He is currently pursuing the Ph.D. degree in intelligent transportation with The Hong Kong University of Science and Technology (Guangzhou), Guangzhou, China. His research interests include intelligent transportation, machine learning, and data analytics.

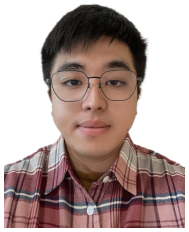

PakHin Tiu graduated with a Bachelor of Science degree in Applied Mathematics, Engineering, and Physics from the University of Wisconsin-Madison, United States, in 2020. He is currently pursuing a Master of Philosophy (MPhil) degree in Intelligent Transportation at the Hong Kong University of Science and Technology (Guangzhou), Guangzhou, China. His research interests encompass intelligent transportation and autonomous driving.

Yihuai Zhang received his B.E. degree in Vehicle Engineering from Southwest University and M.S degree in Vehicle Engineering from South China University of Technology. He is currently pursuing his Ph.D. degree at Intelligent Transportation Thrust, Systems Hub of The Hong Kong University of Science and Technology (Guangzhou). His research interests include PDE boundary control, traffic control and autonomous vehicles.

Xinhu Zheng received the Ph.D. degree in electrical and computer engineering from the University of Minnesota, Minneapolis, in 2022. He is currently an Assistant Professor with the Hong Kong University of Science and Technology (GZ). His current research interests are data mining in power systems, intelligent transportation system by exploiting different modality of data, leveraging optimization, and machine learning techniques.

Meixin Zhu is a tenure-track Assistant Professor in the Thrust of Intelligent Transportation (INTR) under the Systems Hub at the Hong Kong University of Science and Technology (Guangzhou). He is also an affiliated Assistant Professor in the Civil and Environmental Engineering Department at the Hong Kong University of Science and Technology. He obtained a Ph.D. degree in intelligent transportation at the University of Washington (UW) in 2022. He received his BS and MS degrees in traffic engineering in 2015 and 2018, respectively, from Tongji University. His research interests include Autonomous Driving Decision Making and Planning, Driving Behavior Modeling, Traffic-Flow Modeling and Simulation, Traffic Signal Control, and (Multi-Agent) Reinforcement Learning. He is a recipient of the TRB Best Dissertation Award (AED50) in 2023.